AN EXPERIMENTAL PROGRAMME FOR THE DRA MACH SCALED MODEL ROTOR TEST RIG

Dr R H Markiewicz, A F Jones, R J Marshall,
K R Thornton, S P Hill, D J Eckford

Aero-Structures Department, Defence Research Agency
Farnborough, Hampshire, England

Abstract

This paper traces the development and initial application of a new Mach scaled model rotor test rig and describes the main features of the rig, its controls, and the data acquisition and safety monitoring systems currently included. The rig provides the Defence Research Agency, DRA, with an experimental facility for the validation of key areas of new theoretical methods for the prediction of rotor loads and performance and for the safe exploration of new rotor design concepts.

Some initial experiments on isolated rotors are described and discussed showing the practicality of the new facility. Results are shown for the design and successful wind tunnel test of a baseline rectangular blade and an aeroelastically tailored blade incorporating a high performance aerofoil section and a swept tip.

1. Introduction

Massive growth in computing power over the last twenty years has enabled the development of increasingly powerful theoretical methods but the ability to make wind tunnel tests at model scale that are representative of full scale flight remains an essential element in research and development for aerospace vehicles. Rotorcraft constitute a major theoretical and computational challenge and hence, despite inherent engineering difficulties, the achievement of a realistic model test capability in this field is of increasing importance.

Wind tunnel tests on model rotors have been carried out in the Air Systems Sector of the DRA (formerly the Royal Aircraft Establishment, RAE) since the late 1940s, beginning with rudimentary test rigs and wooden rotors of 2-3m diameter. (Refs 1,2 and 3). In the 1970s a rotor rig was designed and built in-house specifically for use in the DRA 24ft (7.3m) wind tunnel, (Ref 4). The rotors were of 3m diameter (later increased to 3.6m) and were mounted at the top of a 4.6m high tower. Collective and cyclic pitch control was through a swashplate system and the rig was driven by 3-phase electric motors through a gearbox below the swashplate and near the top of the tower. The original hub was a semi-rigid type and carried three blades of light alloy and balsa wood construction. Later a new dual-load path hub and composite blades were designed and made in-house along with advances in instrumentation systems. (Ref 5).The rotors used with this rig were dynamically scaled but the correct advance ratio could only be achieved at reduced tip speed (typically 120m/s) as the wind tunnel speed was limited to 40m/s. Hence the effects of compressibility, which affects the advancing blade in particular, could not be simulated.

During the 1980s attention was turned to the provision of a capability for Mach scaled testing. The most suitable available facility where full scale tip speeds could be employed was the DRA 5m low speed wind tunnel where a free stream of Mach 0.3 and a typical full scale tip speed of 220m/s, allow advance ratios up to 0.46 to be obtained. The size and layout of the 5m tunnel and greatly increased power requirements due to Mach scaling meant that a completely new rig was required and the existing in-house capability for the design and manufacture of model blades needed further development. An integrated facility was therefore developed which allows testing at high advance ratios in the DRA 5m wind tunnel, testing at low advance ratio free of constraint effects in the larger 24ft wind tunnel, and hover testing in a purpose built Hover Test Facility. The new rig completed initial commissioning in 1992 and this paper describes the current capability and some of the initial test programme.

2. Rotor test facility

2.1. Rig design philosophy

The rig was designed for use in the 5m DRA wind tunnel at high advance ratios, and in the larger DRA 24ft tunnel at low advance ratios. The rig had to be capable of being mounted in either of these two tunnels and also on a high tower in a purpose built test chamber for out-of-ground-effect hover testing. The rotor tip speed was to be appropriate to full scale helicopters and the rotor diameter was to be as large as the 5m tunnel would allow without excessive interference effects. Provision was also made to drive a smaller rotor diameter at the same tip speed to cater for tilt-rotor applications. The rig was also designed to be self supporting and transportable so that it could be tested in foreign wind tunnels if required. The maximum power requirement was determined by the power needed for stall tests in hover and at high forward speed.

A primary design requirement was the achievement of a configuration allowing both isolated rotor and rotor/fuselage tests, and the ability to separate rotor and fuselage forces and moments in the latter case. This requirement placed stringent limits on cross sectional area of the rig. The design

was to facilitate the measurement of local blade loads and pressures, while accurate measurement of rotor forces and moments dictated that the appropriate balance be mounted as close to the rotor hub as possible.

In order to arrive at the best possible outcome, some existing wind tunnel rotor rigs were examined in the USA and Europe and detailed discussions took place with their users. A firm of engineering consultants also carried out a feasibility study. One conclusion was a preference for electrical rather than hydraulic power provided volume constraints could be met. The two best options for drive arrangement were to have the motor(s) mounted immediately beneath the rotor in a streamlined fairing rather like a fuselage, this being mounted at the top of streamlined column. The other option was to have the power units mounted near the floor of the tunnel with a vertical drive shaft up to the hub at the centre of the tunnel. The former would have precluded isolated rotor configurations while the latter required careful attention to minimise tunnel flow non-uniformities due to asymmetrical tunnel blockage.

2.2. General specifications

The model rig was to consist of the following major assemblies mounted within the tunnel:

Rotor hub.
Rotor blades for commissioning.
Rotor controls (swash plate and associated actuators).
Rotor drive system (shaft, gearbox and drive motors).
Body fairing and rig support structure mounted partially in the tunnel airstream (for the 5m and 24ft wind tunnels).
Force and moment balances within the body fairing.

together with the necessary equipment external to the tunnel such as:

Power supply control units for the drive motors.
Emergency power supplies.
Rig control equipment.

The rig was to be capable of driving a 3m diameter rotor at 1540 rpm and a 2m diameter rotor at 2310 rpm these being the overspeed cases for 1400 and 2100 rpm respectively. A maximum 150 kW was to be available at the rotor. The rotor balance was to be capable of measuring a combined time average and oscillatory thrust load of 8000 N.

The prime contractor for design and manufacture of the rig and the above systems was Advanced Technologies Incorporated (Ref 6) selected by competitive tender.

Development and installation of other sub-systems including:-

Control and monitoring displays.
Data acquisition system.
Mounting stand for operation of the rig at the hover site.
Identical internal data highways at each facility.

was an in-house responsibility.

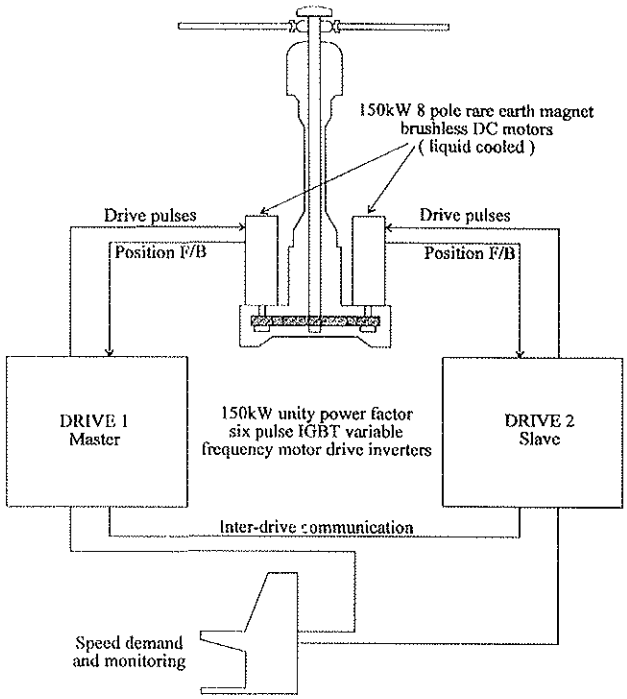

Fig 1 Model helicopter rotor test rig - drive system

2.3. System description

The rotor hub is mounted on a drive shaft assembly, incorporating two flexible couplings, which is connected to the output of the main transmission, Fig 1. The rig is powered by two liquid cooled 150kW, 8 pole, permanent (rare earth) magnet, brushless DC motors, with rotor position feedback for precise control. Each motor is connected to the main transmission via a free wheel clutch unit which serves to mechanically isolate a motor from the transmission in the event of a fault condition occurring in one motor or its drive system. The transmission comprises dual helical pinion gears driving a pair of idler gears which drive a central bull gear connected to the rotor shaft assembly, providing an overall reduction ratio of 2.852 : 1.

2.3.1. Rotor power system The motor drive control system has been designed to provide 150kW of power at the rotor shaft for both 3m and 2m diameter model rotors running at 1400 and 2100 rpm. Each motor is driven by a 180kW, Unity Power Factor Six Pulse Variable Frequency Inverter Drive employing the latest insulated gate bipolar transistors (IGBT) technology. Both drives are identical and are configured to operate as a master slave pair under normal operating conditions. They are commanded from the Rig Operation Console (ROC) via 2 independent fibre optic

digital communication links. Health monitoring, load sharing and current level indications for each drive are displayed on the Rig Safety Monitoring Console (SOC).

An important and vital safety feature of this control system is the capability of either drive to take over from the other in the event of a motor or drive failure and continue to operate the rotor shaft at full power with no reduction in speed, thereby enabling the rig to be shut down in a normal safe controlled manner in unison with wind tunnel air speed. Another safety feature incorporated into this control system is the communications protocol between drives and the control console where each drive monitors the other, if a communications failure is detected between a drive and the console both drives will run off of the other's communications link normally. If all communication is lost with the control console, both drives will continue to operate at their last commanded speed for a pre-set period before ramping down.

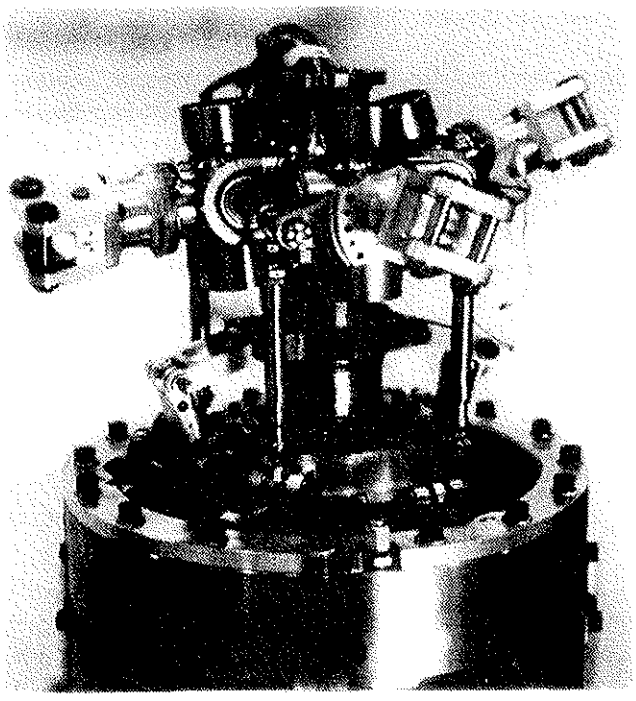

Fig 2 Rotor hub

2.3.2. Rotor control system and pilot console Rotor hubs with three, four, or five blades can be accommodated within the existing swashplate geometry. The existing hub has a conventional articulated system, Fig 2, carrying four blades and has coincident flap and lag hinges at 5% radius. Elastomeric lag dampers which also provide lag spring stiffness are mounted on the lag hinge axis. Interchangeable elastomeric discs enable the stiffness and/or damping to be altered. The collective and cyclic angles of the blades are controlled by pitch links through a swashplate which itself is moved vertically and tilted by three electrically driven actuators attached beneath it at 120 degree intervals.

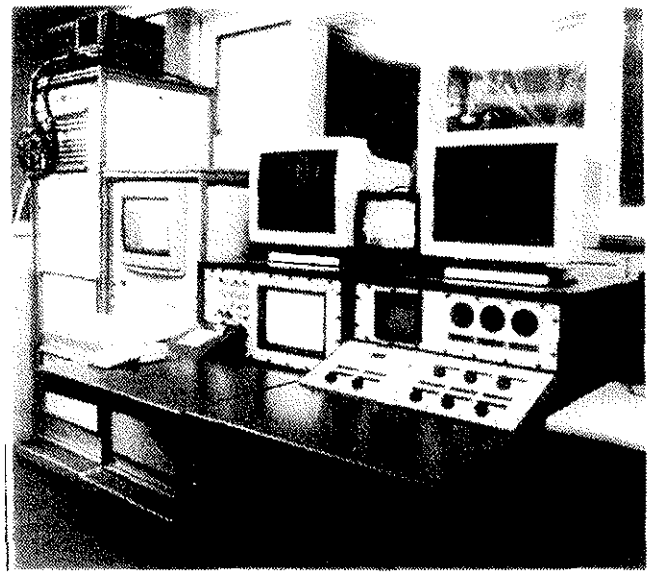

Fig 3 Rotor test rig operator's console

The rig is controlled and flown rather like an actual helicopter. The rotor speed, thrust, cyclic control and shaft tilt are all adjusted to give the required test condition within the prescribed operating limits. The pilot control console, Fig 3, provides the pilot with the controls and displays that are needed to fly the rig safely. The arrangement of the controls and the displays for the pilot are the result of many years of experience with the 24ft wind tunnel rotor rig. The controls are mounted on a sloping panel, on the left of which is mounted the rig rotational speed control. To the right are controls for rotor collective angle, lateral cyclic angle and longitudinal cyclic angles. Above these are further controls for the three swashplate actuators; these are reserved for emergency use in case of actuator failure. All these controls have digital position displays showing the value demanded and the current value. Above the controls on a vertical panel are shown the hub balance horizontal force outputs and analogue and digital displays of rotor rpm, shaft torque and wind tunnel speed.

The signal displays from the rig that the pilot needs in order to be able to fly the rig safely appear on a screen above the manual controls. Various trim strategies are possible but for virtually all tests the rotor is flown in a balanced state with the disc at right angles to the shaft i.e. no 1/rev blade flap angle. Displays include the amount of 1/rev blade flap and the orientation in the form of a vector so that it can be removed by adjusting the cyclic control, the amount of collective as the length of a vertical bar and cyclic as the length and angle of the clock 'hour hand', the flap angle of the master blade against azimuth, the inverted flap angle of the blade on the opposite side of the disc to the master blade, and also alpha numeric displays of rotor rpm, torque and tunnel speed. From his position the pilot can also see the displays on the safety monitor consoles including three video displays showing (a) the rotor blade tips illuminated by a stroboscope so blade tracking can be monitored, (b) a close up of the hub, (c) a wider view showing the rotor and

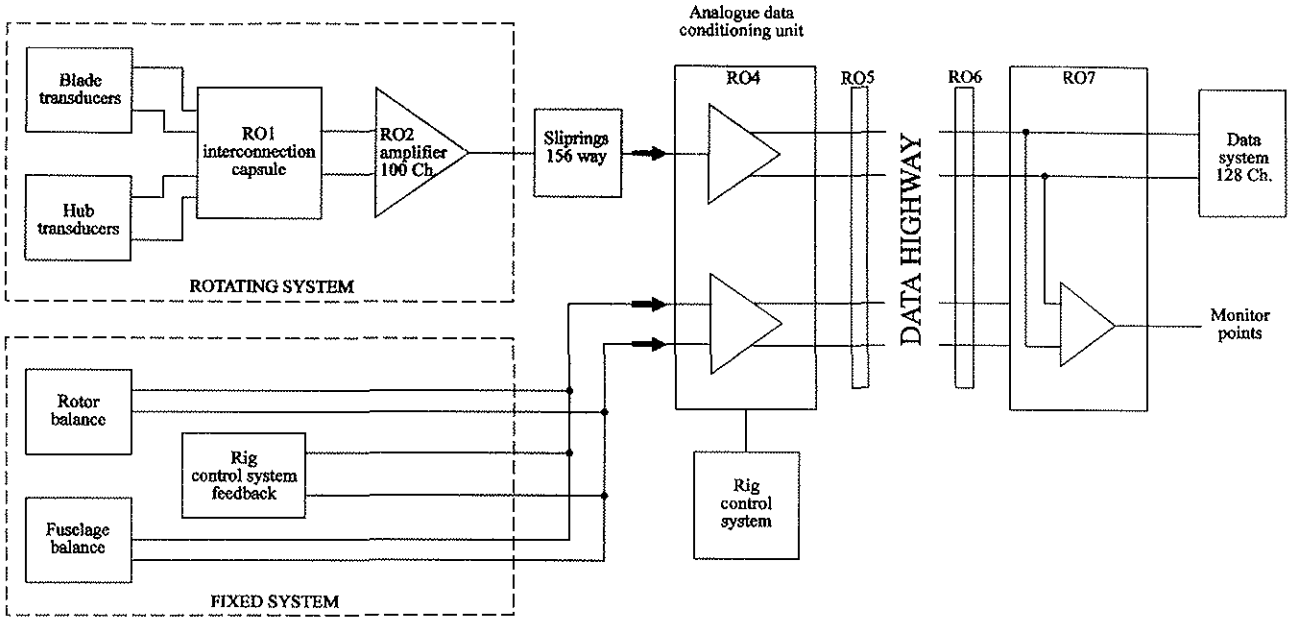

Fig 4 Model helicopter rotor rig - analogue data system

supporting structure. The latter display enables the shaft angle and the local airflow, through the use of tufts, to be monitored.

2.3.3. Signal processing The analogue signal processing system provides excitation and signal conditioning facilities for a wide variety of transducers and transmits analogue data from the test site to the control site, data acquisition, safety monitoring, and operator display systems.

The system comprises 128 channels, of which 100 are available for the rotating system, rotor hub displacement and load transducers and also model rotor blade strain gauges and pressure transducers. The remaining 28 channels are available for the fixed system transducers including the rotor and fuselage load balances and rotor control system actuator transducers.

The main elements of this system are shown in Fig 4 and described below:

a) Interconnection capsule (R01):
Provides a convenient means of connecting differential hub and blade transducers into the rotating system analogue data channels.

b) Shaft mounted amplifier package (R02):
Provides excitation for transducers in the rotating system, facilities for bridge balancing and remotely controlled resistance calibration. The transducer outputs are transformed from differential to single ended, amplified and buffered for passage through the data sliprings.

c) Analogue data conditioning and transmission unit (R04):
Provides excitation, signal conditioning for rotor and fuselage load balances, and other fixed system transducers with facilities for balancing and remote resistance calibration. Rotating system channels received from the shaft mounted amplifier package are transformed from single ended back to differential, all channels are transmitted from the test site to the control site over a data highway.

d) Analogue data monitoring and breakout interface unit (R07):
Receives differential analogue data from R04 and transmits it to the data acquisition and safety monitoring system. Also provides a convenient means of monitoring all analogue data channels via BNC connectors and interfacing to other independent data acquisition and recording devices.

2.3.4. Data acquisition and safety monitoring

2.3.4.1. System definition The data system is required to provide various functions as indicated in Fig 5. The rig operator must be presented with data on current rotor performance which permit him to establish the desired trimmed rotor test condition, and the safety monitor with indications of the loads on the rotor blades and other components in relation to their permissible limits. When the rotor is 'on condition' the data from the various transducers can be recorded. From the combination of these functions the overall system is termed Data Acquisition, Safety Monitoring and Operator Display System (DASMODS).

For the previous rotor test rig developed by RAE the data recording function was performed by a computer-based data acquisition system, the other functions by analogue instrumentation; for the new rig an all-digital system was proposed. The question arose whether a single integrated system should be employed or whether the functions should be implemented separately. The former would clearly ensure complete consistency between the recorded data and that

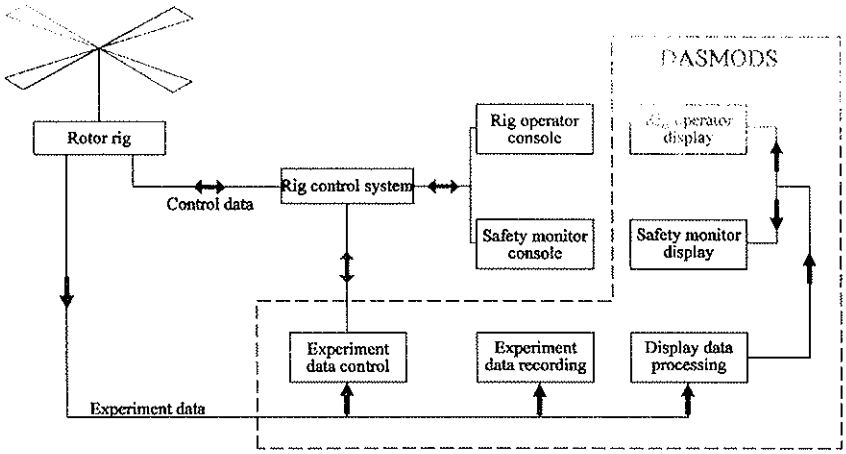

Fig 5 Data Acquisition, Safety Monitoring and Operator Display System functions

presented during rig operation but entailed the greater risk in establishing the performance needed for each function. Similarly, meeting requirements resulting from the specialised nature of the application had to be balanced with the desire to utilise developed sub-systems, thus reducing both risk and cost. The approach adopted was to model the hardware architecture closely on the functional data structure and processes, as shown in Fig 6. Each of the several processors employed could thus be dedicated to a tightly defined set of processes with the advantages that:

a) System performance predictions could be reliably based on individual processor performances.

b) The solution of development problems and provision of future enhancements could concentrate on a limited part of the system, with little concern over side effects.

The successful development and experience to date with the system have validated this approach.

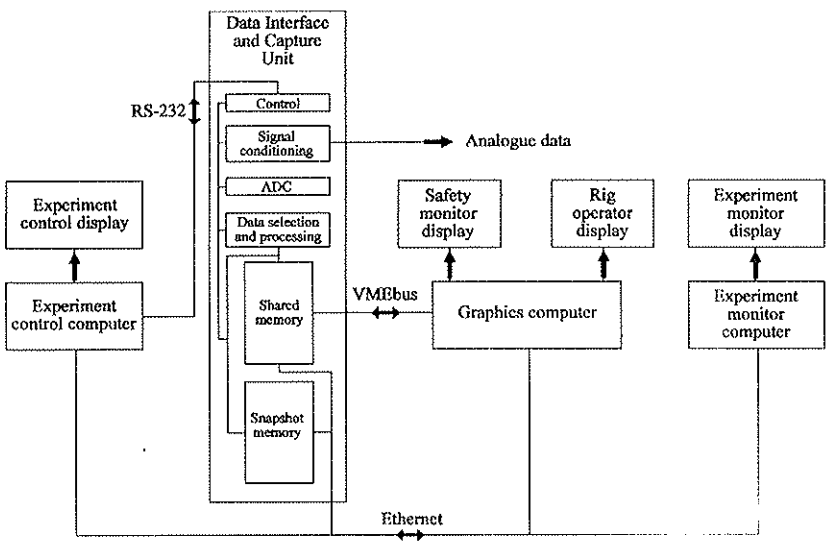

Fig 6 DASMODS architecture

2.3.4.2. Performance requirements The envisaged use of the test rig set the following requirements

128 channels.
256 data points per revolution.
10 000 samples/s data rate per channel acquisition and storage of 32 consecutive revolutions of data per test point.

2.3.4.3. System description There are four main elements:

Data interface and capture unit (DICU).
Experiment control computer.
Graphics computer.
Experiment monitor computer.

The DICU is the heart of the system, providing conditioning of the incoming analogue signals, analogue-to-digital conversion and subsequent selection and processing of the data to be placed in shared memory for access by the graphics computer and in the snapshot memory for the recording of 'on condition' data. The former include the data history for one revolution for up to eight channels and the minimum, the maximum and the mean of the data over one revolution for all channels. For each channel the input gain can be varied between unity and 64, in binary stages. A 8th-order Butterworth filter with selectable cut-off frequency can be applied. A separate ADC is used for each channel. The data acquisition is clocked by a 256/revolution signal derived from the rotor rig and is synchronised to rig rotation by being re-triggered for each revolution by a 1/revolution rig signal.

The experiment control computer provides a graphical interface for the control of the DICU and ancillary equipment which gives an instrument-like 'look and feel' designed around the performance of various operational tasks.

The graphics computer processes the data in shared memory and displays it in formats which are specified by parameters also held in shared memory. The rig operator display typically includes the rotor pitch angles in both numerical and graphical form, a number of data histories and the once-per-revolution frequency component of one of those histories in vector form; driving the vector to zero establishes a trimmed condition. To identify that condition

rotor performance parameters such as C_T/s, C_Q and rotor drive power are displayed. The safety monitor display mainly comprises bars denoting the excursion of chosen quantities over one revolution which are displayed in comparison with the allowable limits of the total quantity and of its fluctuating component; the data history of a single quantity is also displayed.

The experiment monitor computer records the data in the snapshot memory, i e the 'results' for a given test condition, for examination during a test series, for storage and for subsequent analysis.

Of the above elements the first three are 'real-time', providing continuously updated displays for the rig operator and safety monitor, while the experiment monitor computer has only asynchronous access to data via Ethernet - transferring the results for a particular test condition does not interfere with the establishment of the next and does not affect display updating. Thus the efficiency of testing is increased and operational integrity preserved.

2.4. Instrumentation

2.4.1 Rotor and fuselage balances The rotor balance measures five components, the shaft torque being measured by strain gauge bridges on the rotor shaft. The rotor balance is mounted as close to the rotor as possible to minimise corrections due to force displacement. The load carrying capacity of the balance exceeds the normal steady state value in order to cope with potential oscillatory components. The balance consists of two shallow cylinders with their axes vertical joined by four vertical columns. The columns are strain gauged to provide outputs for the three orthogonal components of force and moment. Oil can be circulated through the cylinders ensuring they are at the same temperature and reducing balance drift.

In order to avoid the common problem of a fuselage balance carrying large static loads, particularly bending moments, due to fuselage weight the design employed here consists of two four spoked ring balances equally spaced fore and aft of the rotor shaft. The four spokes are strain gauged and the centres of both four spoke balances are rigidly mounted to the balance support block. The two balance rings are joined by a rigid shell or backbone which can form part of the fuselage. The strain gauge outputs from the eight spokes can be combined to give six component balance outputs.

2.4.2 Other transducers In addition to the hub and fuselage balance transducers the following parameters can also be measured:

a) Shaft angle.
b) Rotor Torque (2 channels).
c) Shaft forces and moments.
d) Flap, lag and pitch angles on the hub.
e) Positions of the three actuators.
f) Transducer data from the blades e.g. strain gauges and pressure gauges.

2.5. Test facilities

2.5.1 Hover test facility The purpose built Hover Test Facility at the DRA, commissioned in 1994, comprises a 15 metre cube in which the rotor rig is mounted on a tower to position the model rotor at a height of 6m above the floor, enabling operation out of ground effect, Fig 7. Peripheral vents at ground and high level can be opened remotely to permit air entry and egress thus resisting recirculation. The facility also includes a large observation / control room, ancillary plant room, calibration room, and fixed data transmission installation identical with that of the two wind tunnels used for rotor testing.

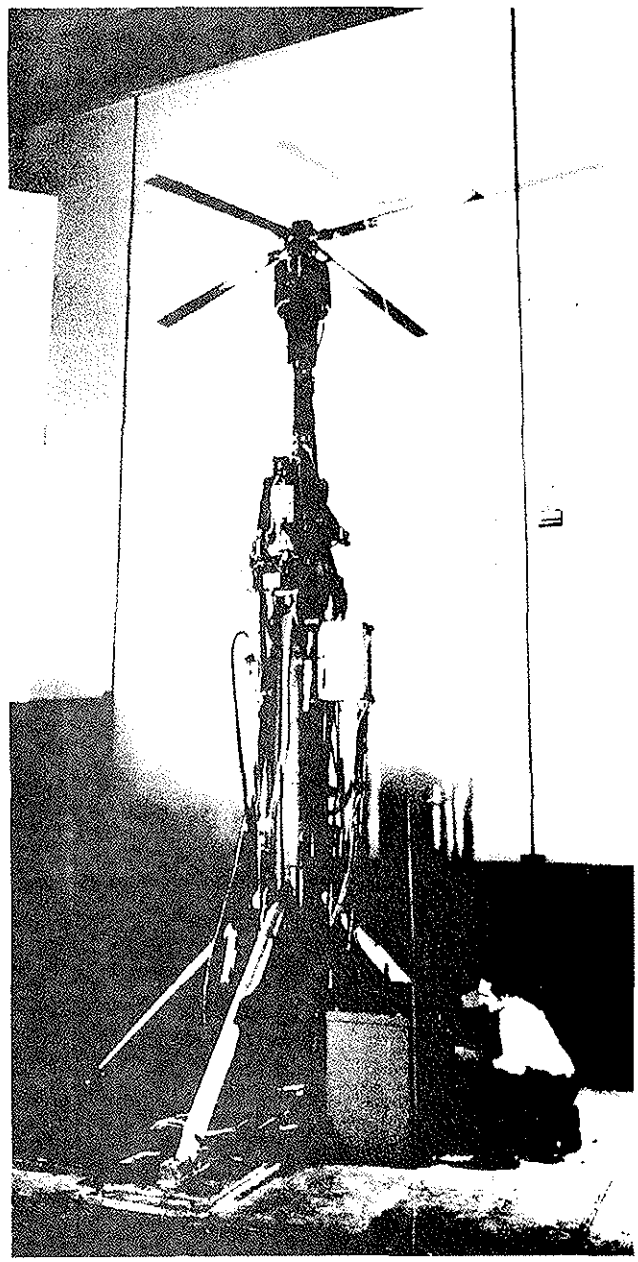

Fig 7 Rotor test rig at the hover facility

2.5.2. 5 Metre Wind Tunnel The DRA 5 Metre wind tunnel is sited adjacent to the Hover Test Facility and has a test section of 5m x 4.2m, and a speed range up to 100m/s at stagnation pressures up to 3 atmospheres. Velocity is uniform to better than 0.05%, temperature stability within 0.5 deg C and rms turbulence level in the range of 0.10 to 0.15%. The tunnel has all of the necessary fixed installations to enable installation of the rotor test rig within 6 working days. Installation is initially to a mobile cart which is driven into the test section when fully prepared.

2.5.3. 24ft Wind Tunnel The DRA 24ft Wind Tunnel has an open jet working section 24 feet in diameter with a large plenum chamber; maximum speed range is 40m/s. It has all of the necessary fixed installations and fittings to enable installation of the Model Helicopter Rotor Test Rig within 10 working days. The tunnel is suitable for model rotor testing up to advance ratios of 0.2 and also acoustic testing.

3. Test programmes

The main experimental programmes for the rig are concerned with validation of theoretical methods for isolated rotors and complete helicopter configurations, and studies of new rotor design concepts. Two such programmes are briefly described here, the first is the investigation of the effects of blade tip aerofoil and planform on vibratory loads and the second is a continuation of earlier successful work on aeroelastic tailoring.

3.1. Blade tip aerodynamics

The results from the flights tests in the British Experimental Rotor Program Phase 3 (BERP3), Ref 7, showed not only an expansion of the flight envelope but also a large reduction in vibration. Cambered aerofoils, which are used on the BERP Lynx, are usually associated with a high stall incidence but can also generate a nose-down pitching moment in transonic conditions. This pitching moment can generate large torsional moments and therefore affect the blade loads. Similarly, a reduced thickness/chord ratio and/or the introduction of sweep, which is used to delay the development of supercritical flow, can affect blade loads. The aim of the programme is to isolate these effects that were combined in BERP3 in order to determine to what extent blade tip planform and aerofoil geometry affects the blade loads and vibration.

Three blade designs are included, Fig 8. The first two blades are of rectangular planform but with different tip sections, each tip providing a different degree of nose-down pitching moment in transonic flow. The final blade design introduces the BERP planform thus exploring the effects of sweep.

The baseline blade, designated blade 1a, has a 0.12m chord, -8 deg. twist and an advanced RAE9646 aerofoil section. The aerofoil section has a high stall incidence, low pitching moment coefficient at low Mach number and a reasonable pitching moment coefficient at high Mach number. The results from wind tunnel tests on blade set 1a serve as a baseline for comparisons with the series of aeroelastically tailored rotor blades.

The second blade, 1b, is the same as the 1a blade out to 84% radius, but the final 5% is replaced by the thinner RAE9634 aerofoil with a linear blend between the two sections. The 9634 section has a lower zero lift pitching moment coefficient at high Mach number. Compared with the BERP3 blade as flown on the Lynx, the transition to the 9634 section is approximately the same as for the model rotor although the transition is over about 2.5% radius for the Lynx.

The final blade, 1c, again has the same section up to 85% as for the 1a blade, but the tip section is replaced by a BERP type tip and the transition from RAE9646 to RAE9634 is over 2.6% radius.

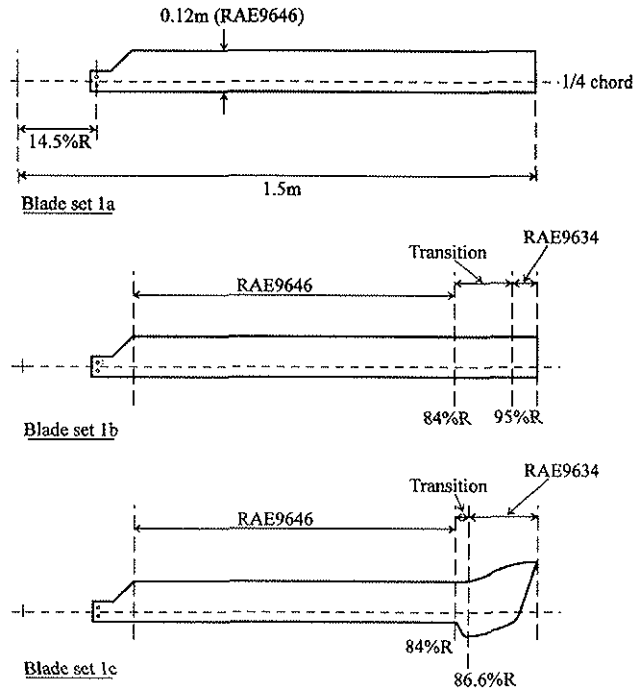

Fig 8 Geometries of the 1a, 1b and 1c rotor blades

3.2. Aeroelastic tailoring

Previous tests on model rotors at the DRA (Refs 8,9), which incorporated aspects of aeroelastic tailoring, showed that blade loads can be reduced and rotor performance improved through the passive variation of blade twist both with azimuth and with forward speed. These results however cannot be extrapolated to the much more difficult dynamic and aerodynamic conditions applicable to full scale, and hence give no guarantee of feasibility of the aeroelastic tailoring concept.

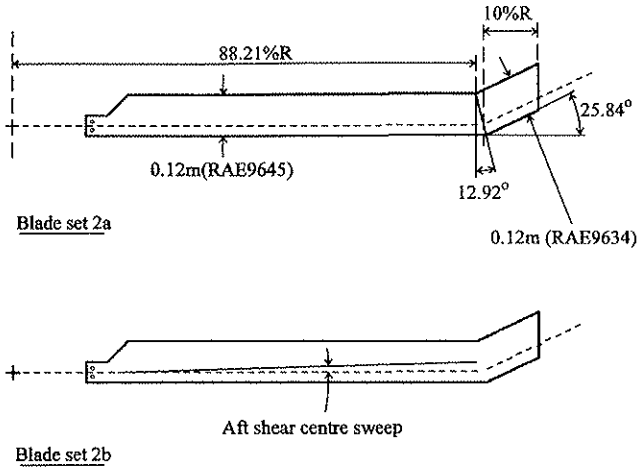

Fig 9 Geometries of the 2a and 2b rotor blades

The current research programme aims to:-

a) Extend the validation of the concept to conditions representative of full scale.

b) Explore by experiment and theory the various forms of coupling appropriate to the design aims.

c) Evaluate the potential of the concept by experiment and theoretical studies.

Two sets of blades incorporate various forms of coupling, Fig 9. Blade 2a has a 10%R swept tip and advanced RAE9645 and RAE9634 cambered aerofoil sections. The chord and radius is the same as for blade 1a. The aim of the swept tip was to provide a torque to the blade which is dependent on the lift on the swept portion. The additional feature of the 2b blade as compared with 2a is the aft sweep of the shear centre relative to the 1/4 chord. The centre of gravity remains on the 1/4 chord thus introducing a flap/torsion inertia coupling. For both the 2a and 2b blades the aim was to explore the two types of coupling without necessarily producing an optimised design.

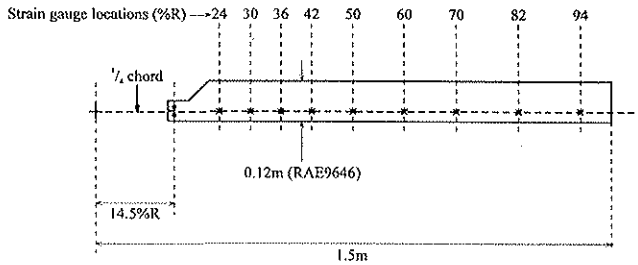

Fig 11 Geometry of the 1a rotor blade showing strain gauge locations

4. The design of blades 1a and 2a

The main design constraints for blade 1a are that the mass must be less than 0.58 Kg/m; the mass limit being imposed by the maximum allowable centrifugal load on the hub, the second flap (2F) frequency must lie between 2.6/rev and 2.8/rev and the first torsion (1T) frequency lies between 5.6/rev and 5.9/rev. Fig 10 shows the predicted spoke diagram for 1a, indicating the correct placement of the 2F and 1T frequencies and showing adequate separation of the

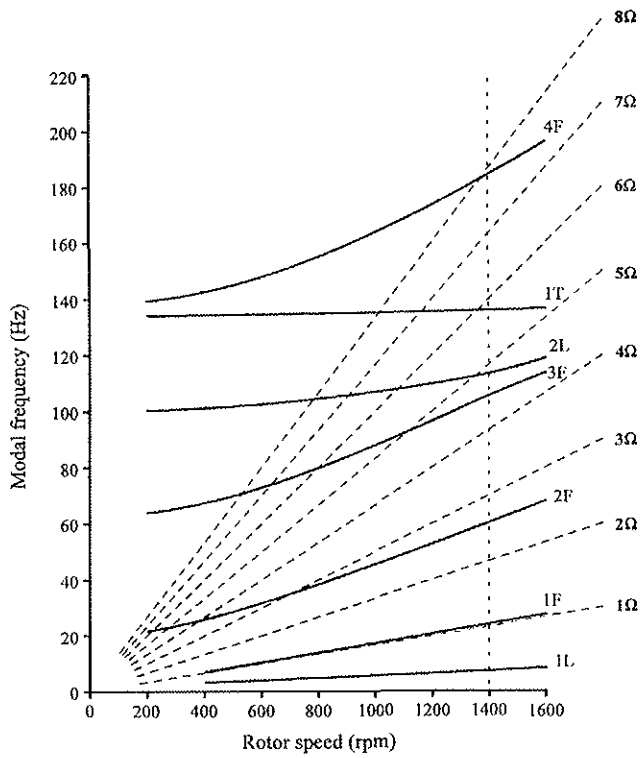

Fig 10 Spoke diagram for blade set 1a

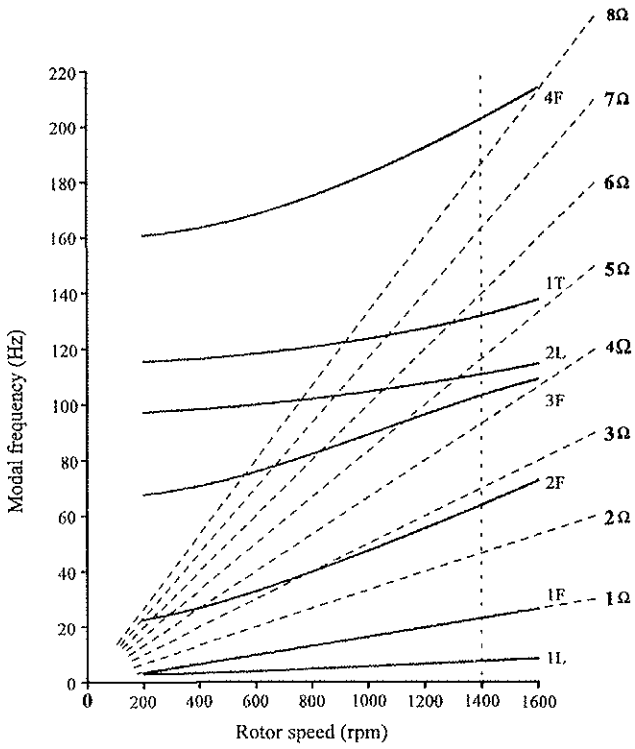

Fig 12 Spoke diagram for blade set 2a

lower order modes from multiples of the normal operating speed. The strain gauge spanwise positions are common between the 1a and 2a blades. Two blades have 9 strain gauge stations positioned between 20% and 95% radius and each station has flap, lag and torsion gauges, Fig 11. Three blades have a set of gauges at only one station.

The 2a blades have similar design constraints to 1a, although the 1T frequency must lie between 5.1/rev and 5.4/rev or between 5.6/rev and 5.9/rev. A theoretical analysis of a prototype design revealed that the additional twist in hover can be in the opposite direction to that found on the previous swept tip blades (Ref 8) and therefore detrimental to rotor performance. The reason is that the dominant force in the twisting of the blade is the component of the centrifugal force acting on the swept tip whilst the blade flaps upwards. This behaviour was avoided by adding a balancing mass at the leading edge just inboard of the swept portion. The spoke diagram for the final design of blade 2a, Fig 12, shows a significant variation in the 1T frequency with rotor speed as compared with blade 1a, Fig 10, indicating a large inertia coupling between the flap and torsion modes despite the added balancing mass. The other 2a modal frequencies shown in Fig 12, except for the fourth flap mode, are similar to those for blade 1a.

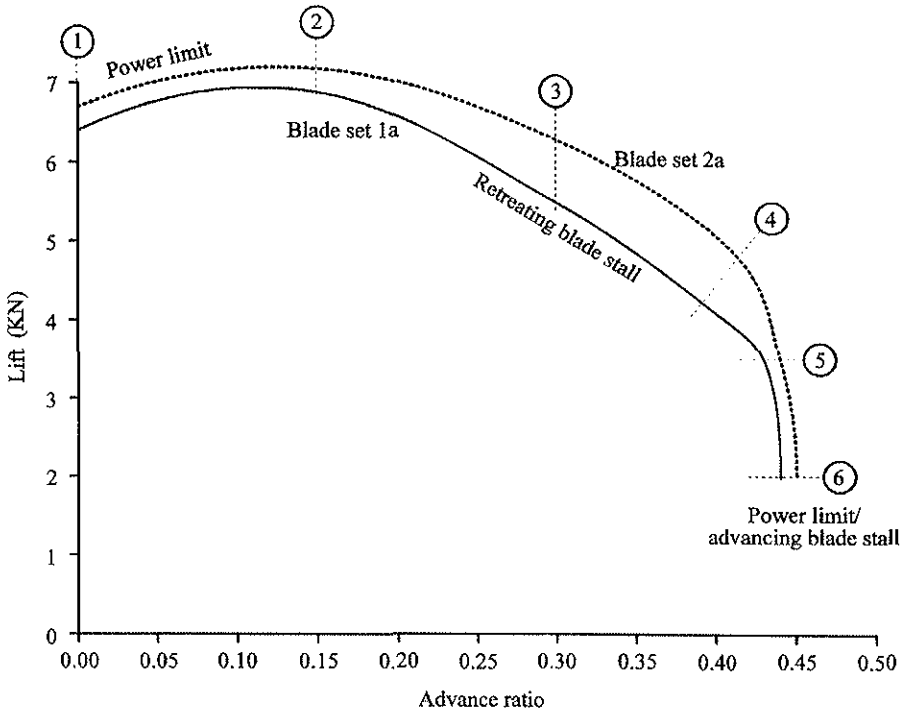

Fig 14 Predicted test envelope for blades 1a and 2a, $\overline{X} = 0.1$

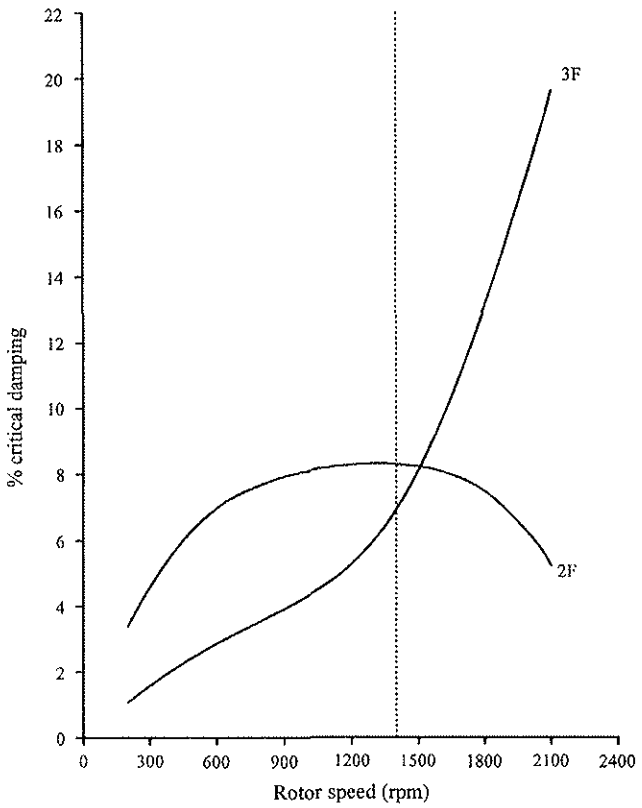

Fig 13 Modal dampings for blade set 2a

An important design issue which arose during the design of the Froude scaled blades with swept tips (Ref 8) is blade stability. Extensive mass balancing had to be incorporated into the blade design to move the overall chordwise centre of gravity nearer the pitch axis. Fig 13 shows that the damping of the second flap mode for blade 2a reduces with rotor speed above 1200 rpm although the blade remains stable at the operating speed and at least up to 2100 rpm.

Fig 14 shows that the predicted test envelope for the 2a blade is significantly larger than for blade 1a. The circled numbers indicate the cases used in determining the shear and moment spectrum for the detailed design and correspond to the case numbers in Figs 15 and 16. Fig 15 shows the predicted peak-to-peak flatwise bending moment for blades 1a and 2a versus spanwise station for a propulsive force coefficient of 0.1. For all cases presented and for most of the spanwise stations, the flatwise moments for 2a are lower than for 1a. Case 1 represents a pseudo-hover case and hence the moments on blade 1a are higher than would be expected in true hover. Fig 16 shows that the predicted 2a torsional moments are lower than on blade 1a only for the lower forward speeds.

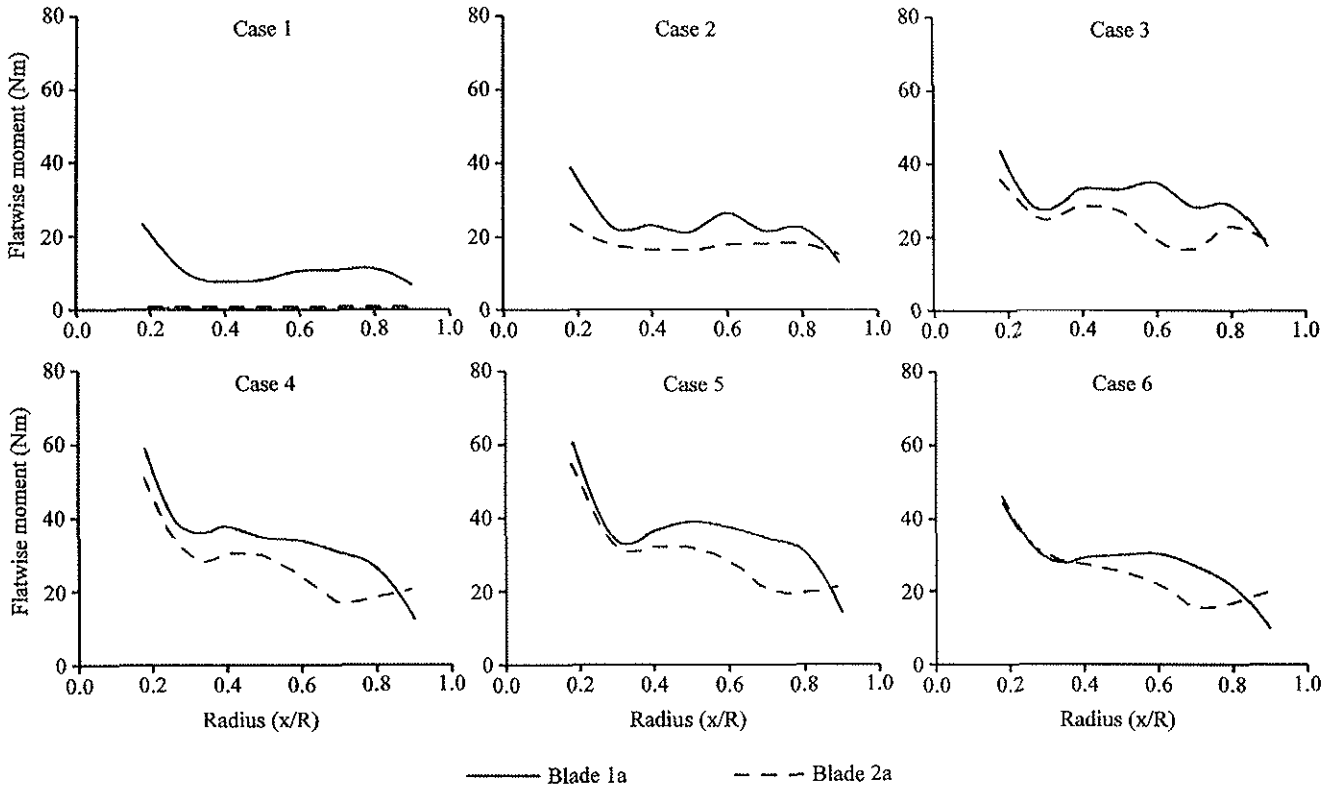

Fig 15 Predicted peak-to-peak flatwise moments for blade sets 1a and 2a, $\bar{\bar{X}} = 0.1$

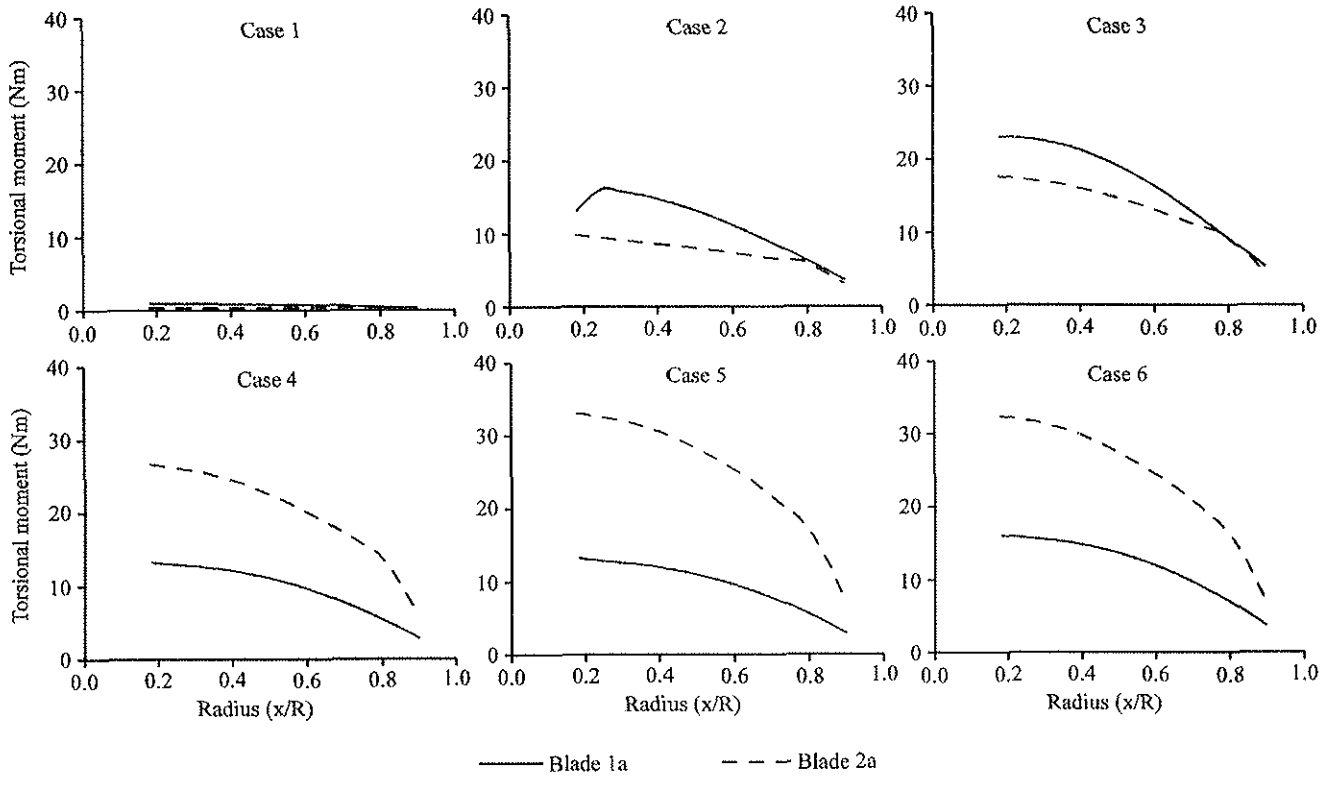

Fig 16 Predicted peak-to-peak torsional moments for blade sets 1a and 2a, $\bar{\bar{X}} = 0.1$

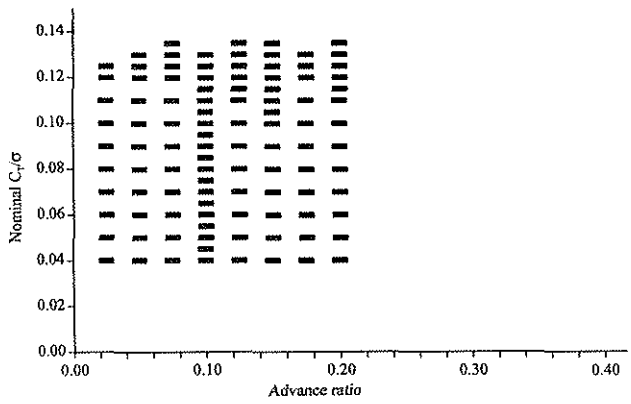

Fig 17 Wind tunnel test conditions for the 1a rotor blade in the DRA 24ft wind tunnel

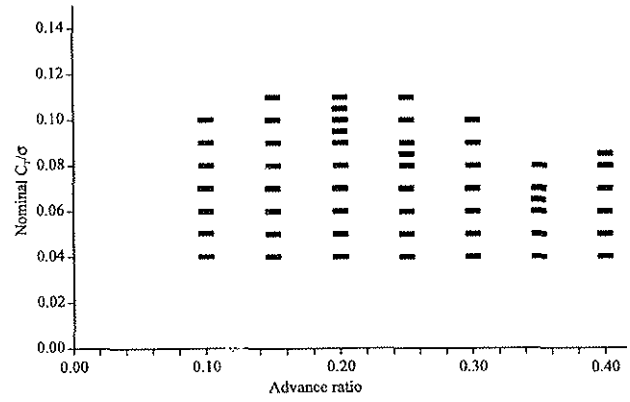

Fig 18 Wind tunnel test conditions for the 1a rotor blade in the DRA 5m wind tunnel

5. The testing of the 1a and 2a rotor blades

The 1a and 2a rotor blades were tested in the DRA 24ft wind tunnel at advance ratios between 0.025 and 0.2 in increments of 0.025 and in the DRA 5m wind tunnel at advance ratios between 0.1 and 0.4. At each of the three shaft angles, 3,6 and 9 degrees forward tilt, the collective was increased to give nominal values of C_T/σ from 0.04 up to the power limit of the rotor rig or until the maximum allowable blade moments were reached. Figs 17 and 18 show the test points for the 1a blades for the 24ft and 5m wind tunnels respectively. Similar test points were recorded for the 2a rotor.

Fig 19 shows the power coefficient plotted against the thrust coefficient divided by the rotor solidity for both the 1a and 2a blade sets. The results are plotted for advance ratios of 0.025, 0.05, 0.1 and 0.2 with the shaft angle set to 3° tilt forwards. In each of the cases presented, and this is true for the other shaft angles tested, the power at a given thrust is lower for 2a than for 1a. The power reduction is up to 6%. The last point taken i.e. at the highest thrust coefficient, does not necessarily suggest that a given level of stall penetration has been achieved. Taking μ=0.1 as an example, the 1a and 2a blades are both at the rig power limit of about 150kW although only the 1a blade loads had reached their maximum allowable. For the other advance ratios presented the 2a tests were terminated when a power of about 130kW was achieved, even though the blade load limits were not reached.

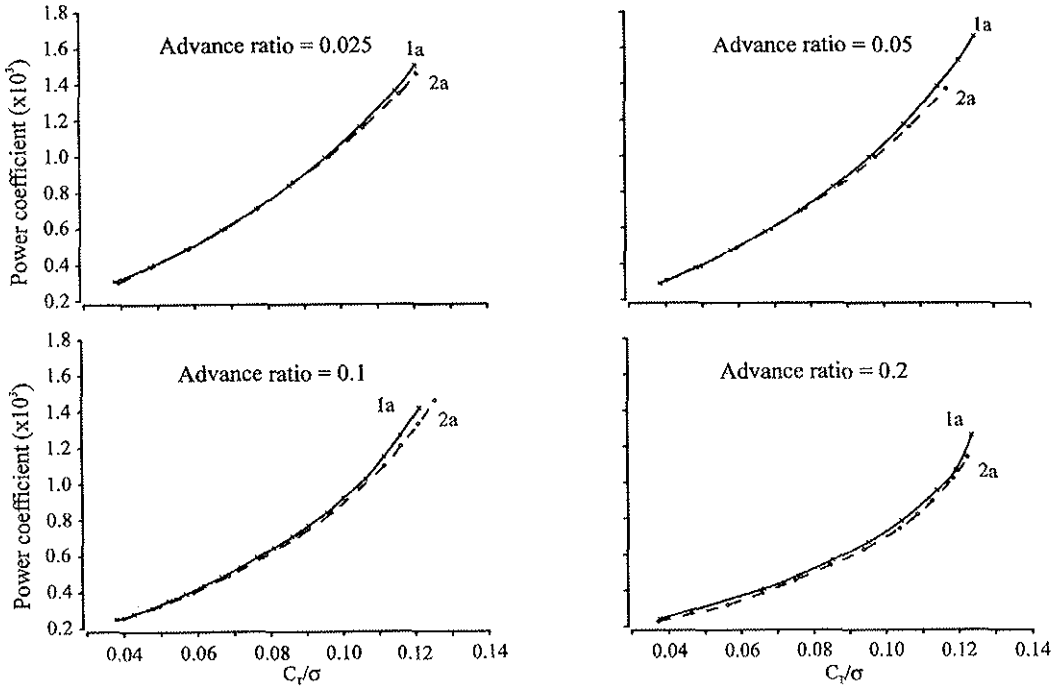

Fig 19 Variation of power coefficient with thrust coefficient for α_s= 3 deg.
- experimental results

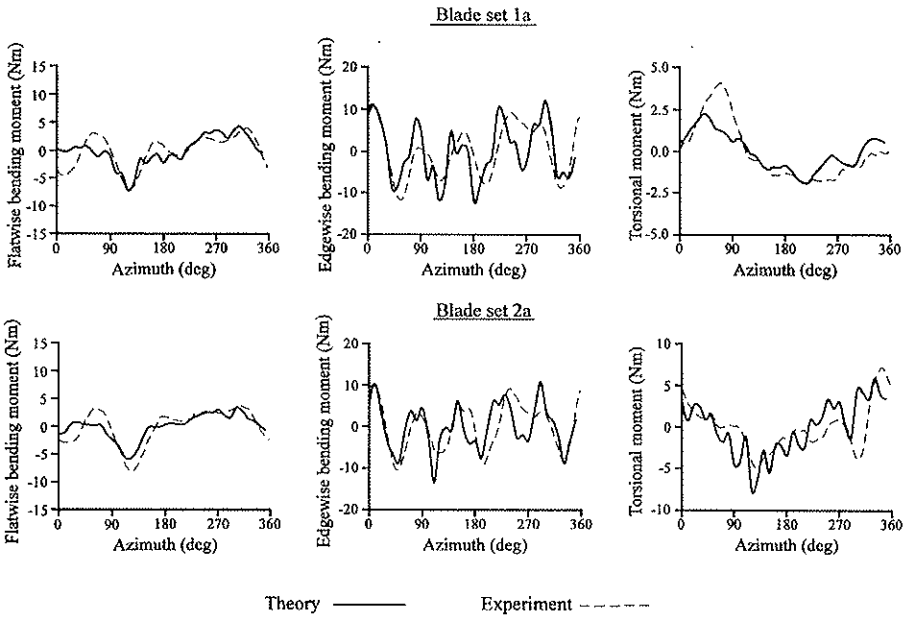

Fig 20 Theoretical and experimental blade moments x = 30%R, $\mu = 0.2$, $C_T/\sigma = 0.1$, $\alpha_s = 3^\circ$

Figure 20 shows comparisons between the measured and predicted flatwise, edgewise and torsional moments respectively, for both the 1a and 2a blades. The results show that there is a reasonable agreement between experiment and theory for both sets of blades and the effects of the swept tip on the torsional moments have been modelled well. Further analysis of the data is required to confirm the level of correlation for other test cases and spanwise stations.

One of the most important aims in aeroelastic tailoring is to change the blade twist both with forward speed and with azimuth. For the hover case predictions show, Fig 21, that the 2a twist should increase with thrust at a higher rate than the 1a blade. A higher thrust should also be achieved by the 2a blade for a given level of stall penetration or power level. Experimental measurements made using a video camera installed at the DRA hover test facility, Fig 22, confirm the theoretical predictions of blade twist.

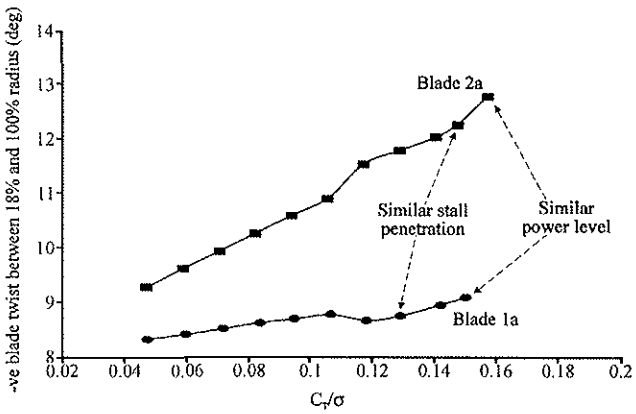

Fig 21 Blade twist predictions (hover)

6. Conclusions

This paper has traced the development and initial application of a new Mach scaled model rotor test rig and described the main features of the rig, its controls, and the data acquisition and safety monitoring systems currently included. The rig provides the DRA with an experimental facility for the validation of key areas of new theoretical methods for the prediction rotor loads and performance and for the safe exploration of new rotor design concepts. The rig and associated test facilities provides an integrated capability for testing isolated rotors and rotor/fuselage combinations in hover, transition and high speed conditions, and for rotor/fuselage combinations allows the separate evaluation of rotor and fuselage forces and moments.

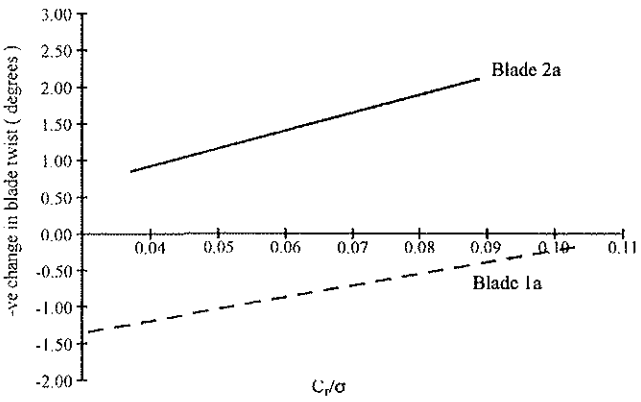

Fig 22 Blade twist measurements (hover)

Some initial experiments on isolated rotors have been described and discussed to show the practicality of the new facility. Results were shown for the design and successful wind tunnel test of a baseline rectangular blade and an aeroelastically tailored blade incorporating a high performance aerofoil section and swept tip. Despite the unconventional design of the aeroelastically tailored blades, they were shown to be stable and the power required was up to 6% lower than for the baseline blade for a given thrust. An initial analysis of the experimental data shows a reasonable agreement with theory.

REFERENCES

1. R A Fail, H B Squire, R C W Eyre, 'Wind tunnel tests on a 12ft helicopter rotor', ARC R&M 2695, April 1949.

2. R A Fail, R C W Eyre, 'Downwash measurements behind a 12ft diameter rotor in the 24ft wind tunnel', ARC R&M 2810, September 1949.

3. T B Owen, R A Fail, R C W Eyre, 'Wind tunnel tests on a 6ft diameter helicopter rotor', ARC CP 216, May 1955.

4. A Anscombe, A P Cox, R J Marshall, 'Wind tunnel testing of model rotors at RAE Farnborough', Paper 34, 2nd European Rotorcraft Forum, 1976.

5. J T Cansdale, R J Marshall, P A Thompson, 'Tests on a new dynamically scaled model rotor in the RAE 24ft wind tunnel', Paper 98, 10th European Rotorcraft Forum 1984.

6. 'Design, manufacture and supply of a model rotor test rig for the 5m Wind Tunnel of the Royal Aircraft Establishment, Farnborough'. Advanced Technologies Incorporated, Proposal P/8916/002.

7. F J Perry, 'Aerodynamics of the helicopter world speed record', 43rd Annual National Forum of the American Helicopter Society, May 1987.

8. R H Markiewicz, 'Theoretical and experimental analysis of a model rotor blade incorporating a swept tip', Paper 49, 14th European Rotorcraft Forum, September 1988.

9. R H Markiewicz, 'A study of the aeroelastic behaviour of helicopter rotor blades featuring swept tips', PhD Thesis, Cranfield Institute of Technology, 1990.